Functional Nanomaterials

DOI: 10.1002/anie.200604973

Redox Luminescence Switch Based on Energy Transfer in $CePO_4$:Tb^{3+} Nanowires**

*Qing Li and Vivian Wing-Wah Yam**

Nanometer-scale devices, as the next generation of optoelectronics as well as biological and chemical sensors, have attracted much attention and been a subject of rapid development recently.[1] Among these devices, fluorescent molecular switches have been attracting great interest because of their outstanding selectivity and the high sensitivity of their luminescence signals, which allow for detection and monitoring at the level of single molecules in solution,[2] as well as for the real-time visualization of cellular events.[3] In addition, the luminescence can be switched on and off easily and rapidly.[4] Recently, much effort has been devoted to molecular switches whose emission properties are influenced by redox processes. Such redox-luminescent switches have been mainly studied by using metal complexes with metal-centered redox couples, in which the communication between the redox-active site (usually a transition-metal complex) and the light-emitting fragment (fluorophore) can switch the light emission on or off.[5] Also, organic-based redox switches have been reported that use, for example, a purely organic couple (quinone/hydroquinone)[6] or tetrathiafulvalene (TTF) as a redox center and free-base porphyrin as a fluorophore.[7] There have also been reports that the redox reaction directly modifies the light-emitting properties of the chromophores in a system that contains 10,10′-dimethylbiacridan, 10-methylacridinium, and acridinium units.[8] However, to the best of our knowledge, the use of rare-earth-metal-centered redox couples as triggers for luminescence switching has not yet been demonstrated. Herein, we describe a facile room-temperature synthetic route to Tb^{3+}-doped $CePO_4$ nanowires. The optical properties of the resulting nanowires were studied, and an interesting enhancement of the energy transfer (ET) induced green emission of the nanowires was observed. Furthermore, a luminescent molecular switch based on the reversible switching of the Ce^{4+}/Ce^{3+} redox couple has been designed and is also described.

Reaction of cerium(III) nitrate and terbium(III) chloride with sodium dihydrogenphosphate in aqueous solution at room temperature in the presence of β-cyclodextrin gave $CePO_4$:Tb^{3+} nanowires in good yield. The chemical reaction involved in the synthesis can be formulated as shown in Equation (1).

$$Ce^{3+} + Tb^{3+} + H_2PO_4^- \rightarrow CePO_4 : Tb^{3+} \downarrow + 2\,H^+ \quad (1)$$

Although a number of synthetic methodologies have been developed to fabricate 1D lanthanide phosphates,[9] they often required relatively high reaction temperatures (100–240 °C), special equipment, or multiple reaction steps. Our method provides a facile and low-cost room-temperature route for the synthesis of Tb^{3+}-doped $CePO_4$ wires of high quality in high yield.

The crystal structure of the product was examined by using X-ray diffraction (XRD). All the diffraction peaks can be well assigned to a hexagonal phase known from bulk $CePO_4$ (JCPDS card, no. 34-1380; see Supporting Information). XRD analyses show slight shifts in the position of the diffraction peaks. The relatively broad XRD peaks reveal the small size of the crystals, and according to the Scherrer diffraction formula the average particle size is approximately 5 nm. The chemical stoichiometry of the as-prepared nanowires was investigated with energy-dispersive X-ray spectrometry (EDX; see Supporting Information), which revealed a molar ratio of Ce, Tb, P, and O close to that employed in the synthesis. This result demonstrates the successful doping of Tb^{3+} in the lattice of $CePO_4$. In addition, the X-ray photoelectron spectroscopy (XPS) data of the as-prepared $CePO_4$:Tb^{3+} sample is in accordance with that reported,[10] which further confirms the elemental composition of the $CePO_4$:Tb^{3+} nanowires.

The morphology and size of the samples was investigated by using scanning electron microscopy (SEM) and transmission electron microscopy (TEM). Figure 1a depicts the field-emission (FE)SEM image, which reveals the chrysanthemum-like architecture of the $CePO_4$:Tb^{3+} crystals. The crystals consist of nanowires as observed from a high-magnification FESEM image (Figure 1b). A typical TEM image of the sample reveals that the as-prepared $CePO_4$:Tb^{3+} wires (Figure 1c) are bent and tangle with each other to form chrysanthemum-like clusters with a uniform size distribution with fibrillar crystallites radiating from the center. From the

[*] Dr. Q. Li, Prof. Dr. V. W.-W. Yam
Centre for Carbon-Rich Molecular and Nanoscale Metal-Based Materials Research and Department of Chemistry
The University of Hong Kong
Pokfulam Road, Hong Kong (P.R. China)
Fax: (+852) 2857–1586
E-mail: wwyam@hku.hk
Prof. Dr. V. W.-W. Yam
Key Laboratory for Supramolecular Structure and Materials of the Ministry of Education
Jilin University
ChangChun 130023 (P.R. China)

[**] V.W.-W.Y. acknowledges support from the University Development Fund and the Faculty Development Fund of the University of Hong Kong, and the University of Hong Kong Foundation for Educational Development and Research, Limited. This work was supported by a grant from the National Natural Science Foundation of China and the Research Grants Council of Hong Kong Joint Research Scheme (NSFC-RGC project no. N_HKU 737/06).

Supporting information for this article is available on the WWW under http://www.angewandte.org or from the author.

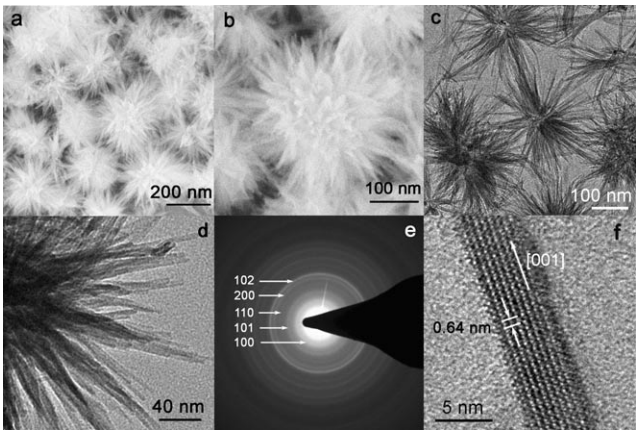

Figure 1. Morphology studies of the $CePO_4$:Tb^{3+} nanowires synthesized at room temperature: a) FESEM image; b) high-magnification FESEM image; c) typical TEM image; d) high-magnification TEM image; e) corresponding electron diffraction patterns; and f) high-resolution TEM image.

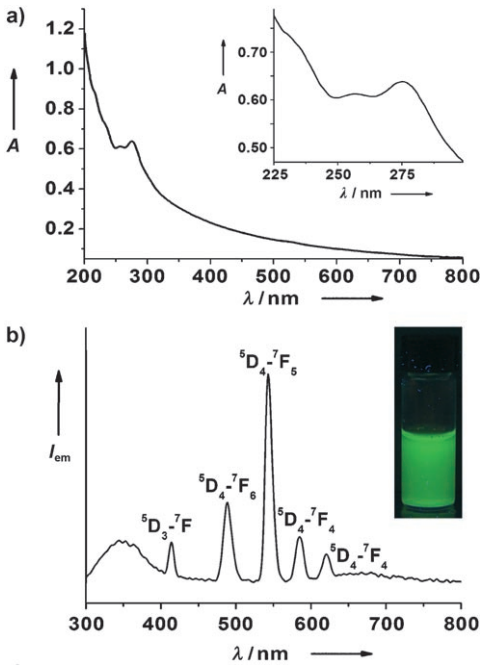

Figure 2. a) UV/Vis absorption and b) room-temperature emission (λ_{ex} = 256 nm) spectra of a dilute colloidal dispersion of $CePO_4$:Tb^{3+} nanowires in ethanol. The inset shows the green (Tb^{3+}) luminescence from the sample recorded with a digital camera.

enlarged image of the wires (Figure 1d), it can be seen that they have a width of about 5 nm and a length of 150–250 nm. Figure 1e shows the selected-area electron diffraction (SAED) patterns obtained by focusing an electron beam onto the wires. From this pattern, the reflections of (100), (101), (110), (200), and (102) planes were clearly seen, indicating that the products are crystalline $CePO_4$:Tb^{3+} nanowires with a hexagonal structural feature, in agreement with the result from XRD measurements. The morphology and microstructure of the as-synthesized products was further investigated in detail by high-resolution (HR)TEM. A representative HRTEM image of randomly selected nanowires (Figure 1f) shows that they are well crystallized without visible defects and dislocations. The calculated interplanar distance is about 0.64 nm, corresponding to the separation of (001) crystal planes. This observation indicates that some of the $CePO_4$:Tb^{3+} nanowires are structurally uniform single crystals with a preferential growth direction of [001] (*c* axis). Compared to the XRD results, as the (100) diffraction peak does not show any changes in intensity the nanowires may exhibit multiple elongation directions.

The growth process of these nanowires was investigated by FESEM, TEM, and XRD techniques. On the basis of the experimental results, the growth of the $CePO_4$:Tb^{3+} nanowires can be divided into three distinctive stages (see Supporting Information). By this route, β-cyclodextrin was found to be the key factor in the anisotropic growth of $CePO_4$:Tb^{3+} nanowires while the pH value of the initial mixture had a significant effect on the shape and size of the resultant nanocrystals (see Supporting Information).

UV/Vis absorption spectra of the crystalline $CePO_4$:Tb^{3+} nanowires show two peaks with maxima at 256 and 273 nm (Figure 2a), consistent with the reported data for 4f–5d electronic transitions for Ce^{3+}.[11] The two bands are overlapped as the excited state is strongly split by the crystal field.[12] Figure 2b shows the room-temperature emission spectrum of a dilute colloidal solution of the $CePO_4$:Tb^{3+} nanowires in ethanol (prepared by ultrasonication to give a transparent and scatter-free solution) upon excitation at 256 nm. It consists of four main peaks between 450 and 650 nm, which correspond to the $^5D_4$–^7F_J transitions of Tb^{3+} ($^5D_4$–$^7F_6$ at 489 nm; $^5D_4$–$^7F_5$ at 543 nm; $^5D_4$–$^7F_4$ at 585 nm; $^5D_4$–$^7F_4$ at 621 nm).[13] Owing to the high concentration of Ce^{3+} in the nanowires, the excited state of Ce^{3+} is not completely quenched by energy transfer to Tb^{3+} and thus its emission (d–f radiative transition) can be seen as a weak broad band between 300 and 400 nm.[14] In addition, an emission peak at 414 nm arising from the $^5D_3$–$^7F_5$ transition for Tb^{3+} is observed.[15] Thus, excitation into the Ce^{3+} band at 256 nm (where Tb^{3+} absorption is negligible)[16] yields the emission typical of both Ce^{3+} and Tb^{3+}. This result indicates that an incomplete energy transfer from Ce^{3+} to Tb^{3+} occurs in the $CePO_4$:Tb^{3+} nanowires, as observed for the bulk powder materials.[17] According to those reports, efficient energy transfer from the broad emitter (i.e. Ce^{3+}) to the narrow-line emitter (i.e. Tb^{3+}) is possible only between nearest neighbors in the crystal lattice and when there is optimal spectral overlap.[17] In the case of Tb^{3+}-doped $CePO_4$ nanowires, the energy levels of Tb^{3+} ($4f^n$) are suitable to accept energy from the excited state of Ce^{3+} following the allowed f–d transition upon its excitation with UV light.[18] The energy-transfer process between Ce^{3+} and Tb^{3+} is schematically depicted in Figure 3. First, Ce^{3+} ions are excited by UV irradiation; then, energy transfer takes place from the $^5D_{3/2}$ state of Ce^{3+} to the acceptor energy states of Tb^{3+}, which decay nonradiatively to the $^5D_4$ and $^5D_3$ states followed by radiative decay to various lower levels of ^7F_J (J = 0–6).[15] As a result, the as-prepared $CePO_4$:Tb^{3+} nanowires show a strong green emission (Figure 2b, inset). The total photolumines-

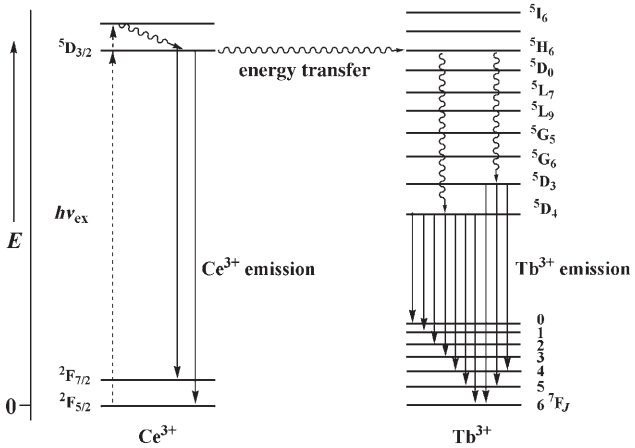

Figure 3. Energy-level diagram of $CePO_4$:Tb^{3+} with radiative transitions and energy-transfer processes. Dashed arrows: excitation; wavy arrows: nonradiative decay; solid arrows: radiative decay.

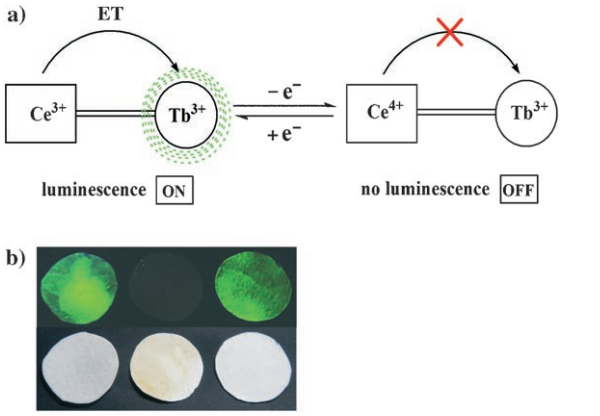

Figure 4. a) Illustration of the redox luminescence switch based on the $CePO_4$:Tb^{3+} nanowires. b) Photographs of samples of $CePO_4$:Tb^{3+} (left), $CePO_4$:Tb^{3+} + $KMnO_4$ (middle), and $CePO_4$:Tb^{3+} + $KMnO_4$ + ascorbic acid (right) impregnated on filter paper with(top) and without (bottom) UV irradiation.

cence quantum yield of the nanowires is around 24%. In such energy-transfer process, the Ce^{3+} ion acts as the sensitizer while Tb^{3+} acts as the acceptor. The emission intensity increases with an increase in Tb^{3+} concentration up to 10%, beyond which the emission tends to be quenched (see Supporting Information). The optimum concentration of Tb^{3+} was found to be 10 mol%.

The luminescence switching behavior was tested by measuring the emission intensity of Tb^{3+} at 543 nm after performing oxidation and reduction of the Ce species. Ascorbic acid is well known to serve as a reducing reagent for Ce^{4+}, while $KMnO_4$ has been successfully employed for the oxidation of Ce^{3+} at room temperature.[19] We found that adding an increasing amount of $KMnO_4$ to the as-prepared $CePO_4$:Tb^{3+} nanowires causes the emission intensity (I_{em}) at 543 nm ($\lambda_{ex} = 256$ nm) to decrease gradually until it is totally quenched (off state).

Subsequent reduction of Ce^{4+} by adding aqueous ascorbic acid to the oxidized solution induced an increase in the luminescence (on state). The redox luminescence switching behavior of $CePO_4$:Tb^{3+} nanowires is illustrated in Figure 4a. Corresponding photographs with and without UV irradiation are shown in Figure 4b. The chemical equations involved in these processes are shown in Equations (2) and (3).

$$3\,Ce^{3+} + MnO_4^- + 2\,H_2O \rightarrow 3\,Ce^{4+} + MnO_2 + 4\,OH^- \quad (2)$$

$$2\,Ce^{4+} + C_6H_8O_6 \rightarrow 2\,Ce^{3+} + C_6H_6O_6 + 2\,H^+ \quad (3)$$

The process is reversible, which means that the luminescence can be switched off and on by the alternate addition of $KMnO_4$ and ascorbic acid to the colloidal dispersion of $CePO_4$:Tb^{3+}. This behavior is in accordance with other kinds of redox switches,[20] in which the luminescence is quenched (off) when the system is in the oxidized form while it is restored (on) in the reduced form.

To demonstrate the reversible switching of the $CePO_4$:Tb^{3+} nanowires, five repeated cycles of oxidation and reduction were performed by the alternate addition of $KMnO_4$ and ascorbic acid. The result demonstrates that the nanowires can be reversibly switched off and on with only a slight degradation of the luminescence intensity in the system (Figure 4b). After the oxidation/reduction sequence $Ce^{3+} \rightarrow Ce^{4+} \rightarrow Ce^{3+}$, no obvious morphological changes of the nanowires was observed by FESEM. The variations in intensity of the strong energy-transfer-sensitized green luminescence are easily visible to the naked eye. These phenomena show the good dispersibility in ethanol of the samples and demonstrate that the system is efficient and versatile and that it may be used as a biological label and probes.

In conclusion, crystalline $CePO_4$:Tb^{3+} nanowires were successfully prepared on a large scale through a facile room-temperature route. This environmentally benign methodology may be extended to the synthesis of other kinds of rare-earth nanoscale materials with or without dopants. The resulting 1D $CePO_4$:Tb^{3+} nanostructures show photoluminescence properties with an enhanced green Tb emission, which was used as a basis to develop a new redox switch that shows a sensitive and prompt response to redox reagents. Owing to its biocompatibility and low toxicity, the system may find applications in biomedical diagnostics and analyses.

Experimental Section

All chemicals were of analytical grade and were used without further purification. Doubly deionized water was used throughout. In a typical procedure, $Ce(NO_3)_3{\cdot}6\,H_2O$ (0.039 g, 0.09 mmol) and $TbCl_3{\cdot}6\,H_2O$ (0.0037 g, 0.01 mmol) were added in a glass beaker (100 mL capacity) containing deionized water (20 mL) and β-cyclodextrin (0.02 g, 0.018 mmol). The mixture was stirred at room temperature for 30 min until a clear solution was obtained. $NaH_2PO_4{\cdot}H_2O$ (0.0276 g, 0.2 mmol) was then added to the reaction mixture, during which the clear solution immediately turned turbid. The mixture was stirred for another 3 h, during which time a white precipitate formed. The solid was collected by centrifugation, washed successively with deionized water and ethanol several times, and dried in air. The final products (over 95% yield, according to the amount of $Ce(NO_3)_3{\cdot}6\,H_2O$ used) were collected for identification and charac-

terization. Details of the XRD, FESEM, TEM, XPS, UV/Vis, and PL apparatus are described in the Supporting Information.

Received: December 8, 2006
Revised: February 14, 2007
Published online: March 30, 2007

Keywords: lanthanides · luminescence · nanostructures · redox chemistry

[1] a) X. Duan, Y. Huang, Y. Cui, J. Wang, C. M. Lieber, *Nature* **2001**, *409*, 66; b) G. M. Whitesides, *Small* **2005**, *1*, 172; c) J. M. Nam, S. I. Stoeva, C. A. Mirkin, *J. Am. Chem. Soc.* **2004**, *126*, 5932; d) S. J. Tans, M. H. Devoret, H. Dai, A. Thess, R. E. Smalley, L. J. Geerligs, C. Dekker, *Nature* **1997**, *386*, 474; e) V. Balzani, A. Credi, M. Venturi, *Molecular Devices and Machines: A Journey into the Nano World*, Wiley-VCH, Weinheim, **2003**.

[2] a) R. Bergonzi, L. Fabbrizzi, M. Licchelli, C. Mangano, *Coord. Chem. Rev.* **1998**, *170*, 31; b) K. Rurack, U. Resch-Genger, *Chem. Soc. Rev.* **2002**, *31*, 116; c) S. Weiss, *Science* **1999**, *283*, 1676; d) J. Andréasson, G. Kodis, Y. Terazono, P. A. Liddle, S. Bandyopadhyay, R. H. Mitchell, T. A. Moore, A. L. Moore, D. Gust, *J. Am. Chem. Soc.* **2004**, *126*, 15926.

[3] P. Yan, M. W. Holman, P. Robustelli, A. Chowdhury, F. I. Ishak, D. M. Adams, *J. Phys. Chem. B* **2005**, *109*, 130.

[4] B. Valeur, *Molecular Fluorescence: Principles and Applications*, Wiley-VCH, Weinheim, **2002**.

[5] a) M. DiCasa, L. Fabbrizzi, M. Licchelli, A. Poggi, D. Sacchi, M. Zema, *J. Chem. Soc. Dalton Trans.* **2001**, 1671; b) L. Fabbrizzi, M. Licchelli, P. Pallavicini, *Acc. Chem. Res.* **1999**, *32*, 846; c) K. Rurack, A. Koval'chuck, J. L. Bricks, J. L. Slominskii, *J. Am. Chem. Soc.* **2001**, *123*, 6205.

[6] V. Goulle, A. Harriman, J. M. Lehn, *J. Chem. Soc. Chem. Commun.* **1993**, 1034.

[7] H. Li, J. O. Jeppesen, E. Levillain, J. Becher, *Chem. Commun.* **2003**, 846.

[8] T. Suzuki, A. Migita, H. Higuchi, H. Kawai, K. Fujiwara, T. Tsuji, *Tetrahedron Lett.* **2003**, *44*, 6837.

[9] a) H. Meyssamy, K. Riwotzki, A. Kornowski, S. Naused, M. Haase, *Adv. Mater.* **1999**, *11*, 840; b) Y. Fang, A. Xu, W. Dong, *Small* **2005**, *1*, 967; c) C. Tang, Y. Bando, D. Golberg, R. Ma, *Angew. Chem.* **2005**, *117*, 582; *Angew. Chem. Int. Ed.* **2005**, *44*, 576; d) W. Bu, H. Chen, Z. Hua, Z. Liu, W. Huang, L. Zhang, J. Shi, *Appl. Phys. Lett.* **2004**, *85*, 4307.

[10] J. M. Pemba-Mabiala, M. Lenzi, J. Lenzi, A. Lebugle, *Surf. Interface Anal.* **1990**, *15*, 663.

[11] Z. Wang, Z. Quan, J. Lin, J. Fang, *J. Nanosci. Nanotechnol.* **2005**, *5*, 1532.

[12] K. Riwotzki, H. Meyssamy, A. Kornowski, M. Haase, *J. Phys. Chem. B* **2000**, *104*, 2824.

[13] U. Rambabu, N. R. Munirathnam, T. L. Prakash, S. Buddhudu, *Mater. Chem. Phys.* **2003**, *78*, 160.

[14] K. Kömpe, H. Borchert, J. Storz, A. Lobo, S. Adam, T. Möller, M. Haase, *Angew. Chem.* **2003**, *115*, 5672; *Angew. Chem. Int. Ed.* **2003**, *42*, 5513.

[15] M. T. Jose, A. R. Lakshmanan, *Opt. Mater.* **2004**, *24*, 651.

[16] J. C. Bourcet, F. K. Fong, *J. Chem. Phys.* **1974**, *60*, 34.

[17] N. Hashimoto, Y. Takada, K. Sato, S. Ibuki, *J. Lumin.* **1991**, *48–49*, 893.

[18] S. Redei, F. W. Ainger, D. Ravichandran, W. B. White, *Mate. Lett.* **1997**, *30*, 389.

[19] a) S. M. Sultan, Y. A. M. Hassan, K. E. E. Ibrahim, *Analyst* **1999**, *124*, 917; b) Y. Miura, M. Hatakeyama, T. Hosino, P. R. Haddad, *J. Chromatogr. A* **2002**, *956*, 77; c) I. M. Issa, M. G. E. Allam, *Fresenius Z. Anal. Chem.* **1961**, *182*, 244; d) K. A. Idriss, I. M. Isse, Y. M. Temerk, *Z. Anal. Chem.* **1976**, *278*, 364.

[20] a) R. Bergonzi, L. Fabbrizzi, M. Licchelli, C. Mangano, *Coord. Chem. Rev.* **1998**, *170*, 31; b) V. Goulle, A. Harriman, J. M. Lehn, *J. Chem. Soc. Chem. Commun.* **1993**, 1034.

